Hindawi
Mathematical Problems in Engineering
Volume 2020, Article ID 9730129, 12 pages
https://doi.org/10.1155/2020/9730129

Research Article

The Impact of Different Mapping Function Models and Meteorological Parameter Calculation Methods on the Calculation Results of Single-Frequency Precise Point Positioning with Increased Tropospheric Gradient

Ying Liu,[1] Ren Wang,[1,2] Jingxiang Gao,[2] and Peng Zhu[1]

[1]*School of Marine Technology and Geomatics, Jiangsu Ocean University, Lianyungang 222000, China*
[2]*School of Environment Science and Spatial Informatics, China University of Mining and Technology, Xuzhou 221116, China*

Correspondence should be addressed to Ren Wang; chwangr1990@163.com

Received 21 June 2020; Accepted 20 August 2020; Published 6 October 2020

Academic Editor: Filippo Cacace

Tropospheric delay is one of the main errors in precise point positioning (PPP). The inaccuracy of the tropospheric delay model will inevitably lead to a decrease in PPP accuracy. Therefore, the influence of the tropospheric gradient on the positioning accuracy should be considered in the processing of tropospheric delay. At the same time, the effects of different mapping function models and meteorological parameter calculation methods on the tropospheric delay accuracy of single-frequency PPP (SF PPP) are analyzed. Twelve MGEX stations, which are evenly distributed in the world, are used in this article. Taking into account the seasonal variation of the tropospheric delay, the observation times adopted are 2016, 2017, and 2018 for different seasons (winter, day of year (DOY): 22–28; spring, DOY: 92–98; summer, DOY: 199–205; and autumn, DOY: 275–281). Then, according to different mapping function models and meteorological parameter calculation methods, a total of 7056 tests and 9072 tests are performed, respectively. The following results were obtained after comparative analysis. (1) When the same method is used for calculating meteorological parameters, the percentage with improved tropospheric delay repeatability calculated by the Hopfield mapping function model (MFM3) is the highest, reaching more than 70%, and by Vienna Mapping Functions 3 (VMF3, grid resolution is 1°), the mapping function model (MFM8) is the lowest, less than 67.5%. The percentage with improved position repeatability is highest in the north (N) direction and lowest in the up (U) direction. (2) Using the same mapping function model, the correction of the tropospheric gradient model has a greater impact on calculating the repeatability percentage of the tropospheric delay and the position. Compared with standard atmospheric parameters, other calculation methods of meteorological parameters have little effect on the percentage increase of the tropospheric delay value and the positioning result after adding the tropospheric gradient model. It shows that different calculation methods of meteorological parameters have little effect on the calculation of tropospheric delay and position, different mapping function models have a large effect on the calculation of tropospheric delay and position, and the tropospheric gradient model has the greatest influence on the calculation of tropospheric delay and position.

1. Introduction

The electromagnetic signal sent by the satellite to the ground receiving equipment must pass through the troposphere. Because the troposphere is nondispersive [1], there will be a delay in the process of electromagnetic propagation, and this delay cannot be reduced by a combination method like the ionosphere delay. The tropospheric delay can reach 2.3 m in the zenith direction and can reach 20 m at low-elevation angle [2], which depends on pressure, temperature, and humidity along the path of the signal transmission. This value will affect the accuracy of global navigation satellite system (GNSS) positioning, so it is necessary to correct it.

Zenith tropospheric delay (ZTD) consists of two parts: zenith hydrostatic delay (ZHD) and zenith non-hydrostatic delay (zenith wet delay, ZWD). Meteorological data are used

in calculating the ZHD and ZWD [3]. It is necessary to accurately estimate the meteorological data. Boehm et al. [4] developed an empirical global pressure and temperature (GPT) model, which is based on a ninth-order spherical harmonic and can provide pressure and temperature anywhere near the surface of the Earth. Because of the limited spatial and temporal variability of the GPT model, Lagler et al. [5] proposed the global pressure and temperature 2 (GPT2) model, which is a combination of GPT and GMF (global mapping function) models [6]. The GPT2 model can provide pressure, temperature, lapse rate, water vapor pressure, and mapping function coefficients at any site, resting upon a global 5° grid. On the basis of GPT2, Boehm et al. [7] further improved the gradient fitting terms of water vapor pressure, air temperature, and air pressure and proposed the global pressure and temperature 2 wet (GPT2w) model.

ZHD and ZWD are both delays in the zenith direction, which needs to be converted to the signal propagation path direction and then requires a mapping function. In navigation, when electromagnetic signals pass through the atmosphere, complete X-ray tracing should be used to describe their walking trajectories. For convenience, they can be described by analytical functions, which are also mapping functions. In general, with the tropospheric delay at a given zenith angle (φ), Saastamoinen [8] proposed a simple $1/\cos\varphi$ mapping function in 1972. This simple mapping function was found to be quite suitable for estimating the slant delay of zenith angles up to 70°. For higher zenith angles, this function will severely fail [1]. Under the large zenith angle, Marini [9] proposed that mapping function can be approximated as a continuous fraction. Herring [10] had developed a new set of mapping functions based on the continued fraction form, which was developed by ray tracing through atmospheres with temperature and water vapor. Niell [11] had used the temperature and relative humidity of the mapping function based on the continued fraction form. In addition, in 2000, Niell [12] proposed a new mapping function based on in situ meteorological parameters, which is used to calculate the length of the radio path through the atmosphere when the elevation is as low as 3°. It includes a hydrostatic mapping function and a wet mapping function. Foelsche and Kirchengast [13] proposed a simple mapping function in which the only parameter is the "effective height" of the atmosphere, which is also the continued fraction form. Younes [14] provided a new mapping function that has better low-elevation performance over a range of up to 5°. Of course, there are many other mapping functions that will be presented in the following section [6, 11, 15–18].

This article mainly studies the effects of tropospheric gradient, different mapping functions, and meteorological data calculation methods on tropospheric delay based on single-frequency (SF) precise point positioning (PPP). SF PPP does not need to eliminate or weaken some observations through difference and combination to make the observation information more abundant, such as ionospheric delay information. The organization of this article is as follows: next, the tropospheric wet delay, tropospheric dry delay and tropospheric gradient models, 9 tropospheric delay projection function models, and 7 meteorological parameter calculation methods are introduced in detail. Then, in Section 3, the effects of the tropospheric gradient model, different mapping function models, and meteorological parameter calculation methods on tropospheric delay and position are analyzed, and we finally give the conclusions in Section 4.

2. Methods

The ZHD model, ZWD model, and tropospheric gradient model are first derived. Then, different mapping function models are analyzed. Finally, different ways of obtaining meteorological parameters such as pressure and temperature are introduced.

2.1. ZHD and ZWD Models. The undifferenced and uncombined GNSS PPP model uses pseudorange and carrier phase observations, with the following expression [19, 20]:

$$\begin{cases} P_r^s = \rho_r^s + c\cdot\left(\mathrm{d}t_r - \mathrm{d}t^s\right) + I_r^s + T_r^s + d_r - d^s + \varepsilon_r^s, \\ L_r^s = \lambda_1\cdot\Phi_r^s, \\ = \rho_r^s + c\cdot\left(\mathrm{d}t_r - \mathrm{d}t^s\right) - I_r^s + T_r^s + \lambda_1\cdot\left(N_r^s + b_r - b^s\right) + \xi_r^s, \end{cases} \tag{1}$$

where P_r^s is the pseudorange and L_r^s is obtained by multiplying the carrier phase Φ_r^s and the wavelength λ_1 for the specific receiver r and satellite s; ρ_r^s is the geometric distance from the receiver r to satellite s; c is the speed of light in vacuum; $\mathrm{d}t_r$ and $\mathrm{d}t^s$ are the clock error of the receiver and satellite; I_r^s is the slant ionospheric delay on the first frequency f_1; T_r^s is the tropospheric delay; d_r is the frequency-dependent receiver uncalibrated code delay (UCD) with respect to satellite s; d^s is the frequency-dependent satellite UCD (since the satellite clock offset $\mathrm{d}t^s$is linearly dependent with the satellite UCD d^s in (1), the satellite UCD cannot be directly isolated from the satellite clock offset without additional constraints; for specific treatment methods, please refer to reference [19]); N_r^s is the integer phase ambiguity; b_r and b^s are the uncalibrated phase delays (UPDs) for the receiver and satellite, which is frequency dependent; and ε_r^s and ξ_r^s are the sum of measurement noise caused by the pseudorange and carrier phase observations and the error caused by the multipath effect. Other errors have been modeled in advance.

When electromagnetic waves pass through the neutral atmosphere, a tropospheric delay is generated, and the tropospheric delay includes tropospheric dry delay and wet delay. When the elevation angle of electromagnetic wave propagation is θ, the resulting tropospheric delay can be expressed as follows:

$$T_r^s = T_h^z\cdot MF_h(\theta) + T_w^z\cdot MF_w(\theta), \tag{2}$$

where $T_i^z\,(i = h, w)$ is the delay of the troposphere in the direction of the zenith; $MF_i\,(i = h, w)$ is a mapping function; T_h^z is a hydrostatic part of the tropospheric delay, which is

mainly caused by the dry gases in the atmosphere; and T_w^z is a wet part which arises from water vapor in the atmosphere. By inputting meteorological parameters of the station, the tropospheric dry delay can be calculated with a model to achieve very high accuracy. There are many dry delay calculation models. The Saastamoinen [8] model is selected here, and its expression is as follows:

$$T_h^z = \frac{0.0022768 \cdot P}{1 - 0.00266 \cdot \cos(2\varphi) - 0.28 \cdot 10^{-6} \cdot h_{\text{ell}}}, \quad (3)$$

where P is the pressure and φ and h_{ell} are the geographic latitude and ellipsoidal height of the station, respectively.

Because of the high variability of meteorological parameters in both spatial and temporal domains [21], the tropospheric wet delay cannot be obtained by establishing the accuracy of the model. Therefore, in high-precision GNSS applications, wet delay is generally considered as the parameter to be estimated.

Substituting equations (2) and (3) into equation (1)fd1, the linearized observation model can be rewritten as follows:

$$\begin{bmatrix} p_r^1 \\ l_r^1 \\ \vdots \\ p_r^m \\ l_r^m \end{bmatrix} = \begin{bmatrix} -\mu_r & I_t & MF_w & K & R \end{bmatrix} \begin{bmatrix} x \\ \mathrm{d}\bar{t}_r \\ T_w^z \\ I_r^s \\ \overline{N}_r^s \end{bmatrix} + \begin{bmatrix} \varepsilon_r \\ \xi_r \end{bmatrix}, \quad Q_L, \quad (4)$$

where μ_r is the unit vector of the coordinate component between the receiver and the satellite; x is the vector of the receiver position increments relatively to the priori position; and I_t is a unit vector of $2 \cdot m$ rows and one column, corresponding to the receiver clock parameter $\mathrm{d}\bar{t}_r$. In matrix K, the elements for the corresponding p_r^s and l_r^s are 1 and −1, respectively, corresponding to the ionospheric parameter I_r^s. R is the matrix corresponding to the ambiguity parameters $\overline{N}_r^s$, and the elements for the corresponding p_r^s and l_r^s are 0 and 1, respectively. Q_L is the stochastic model of the observed minus computed (OMC) observables.

When the tropospheric delay is taken into account, the tropospheric gradient, equation (2), is rewritten as follows [22];

$$\begin{aligned} T_r^s = {} & T_h^z \cdot MF_h(\theta) + T_w^z \cdot MF_w(\theta) + MF_g(\text{el}) \\ & \cdot \left[G_{\text{ns}} \cdot \cos(\text{az}) + G_{\text{ew}} \cdot \sin(\text{az})\right], \end{aligned} \quad (5)$$

where el and az are the elevation and azimuth angle of the satellite, respectively, $MF_g(\text{el})$ is the gradient mapping function [23], and G_{ns} and G_{ew} are the gradient vectors with north-south and east-west components, respectively.

Then, equation (4) can be rewritten as follows:

$$\begin{bmatrix} p_r^1 \\ l_r^1 \\ \vdots \\ p_r^m \\ l_r^m \end{bmatrix} = \begin{bmatrix} -\mu_r & I_t & MF_w & I_g & K & R \end{bmatrix} \begin{bmatrix} x \\ \mathrm{d}\bar{t}_r \\ T_w^z \\ G_g \\ I_r^s \\ \overline{N}_r^s \end{bmatrix} + \begin{bmatrix} \varepsilon_r \\ \xi_r \\ \varepsilon_g \end{bmatrix}, \quad Q_L, Q_G, \quad (6)$$

where $G_g = \begin{bmatrix} G_{\text{ns}} & G_{\text{ew}} \end{bmatrix}^T$, I_g is a matrix of $2 \cdot m$ rows and two columns in which all elements are 1, corresponding to the gradient vector G_{ns} and G_{ew}, ε_g is the noise of gradient, and Q_G is the stochastic model of the gradient vector.

2.2. Mapping Function Models. Because of the large number of calculations and limitations of the paper length, results of various mapping functions will be analyzed later; interested readers can refer to the references in the first column of Table 1 for details about the principles, methods, and formulas of mapping functions. The table gives the input parameters required for each model and clarifies the conditions under which each model is used.

2.3. Different Methods for Obtaining Meteorological Parameters. Since the meteorological parameter is used in the calculation of the dry delay and the initial values of the wet delay, this paper summarizes and analyzes several meteorological methods in Table 2.

3. Experiment and Analysis

In order to verify the influence of mapping function and meteorological parameter calculation method on the tropospheric delay, the tropospheric delay product published by IGS was taken as the reference true value. Taking into account the seasonality of the tropospheric delay, 2016, 2017, and 2018 data for different seasons (winter, day of year (DOY): 22–28; spring, DOY: 92–98; summer, DOY: 199–205; and autumn, DOY: 275–281) [24] were used to evaluate the tropospheric delay and position of different models. The distribution of the 12 MGEX (Multi-GNSS Experiment) tracking stations used is shown in Figure 1, and Figure 2 shows the processing flow of the article.

For the convenience of expression, different mapping function models and meteorological parameter calculation methods are abbreviated, as shown in Table 3.

Table 1: The properties of different troposphere mapping functions.

Mapping function	Reference	Input parameters	Output parameters
B&E	Black and Eisner [15]	θ	mf_h, mf_w
GMF	Boehm et al. [6]	$\theta, d_{\mathrm{mjd}}, \phi, h, \lambda$ and ERA-40 data at $15^\circ \times 15^\circ$grid	mf_h, mf_w
Hopfield	Hopfield [16]	P, T, θ	mf_h, mf_w
NMF	Niell [11]	θ, DOY, ϕ, h	mf_h, mf_w
VMF1_site	Boehm et al. [6]	$\theta, d_{\mathrm{mjd}}, h, \phi, a_h, a_{w,\mathrm{VMF1\ site\ file}}$	mf_h, mf_w
VMF1_grid	Niell [11] and Kouba [17]	$\theta, d_{\mathrm{mjd}}, h, \phi, \lambda_{,\mathrm{VMF1\ gridded\ file,\ orography\_ell\ file}}$	mf_h, mf_w, zhd, zwd
VMF3_site	Landskron and Bohm [18]	$\theta, d_{\mathrm{mjd}}, h, \phi, \lambda, a_h, a_{w,\ \mathrm{VMF3\ site\ file}}$	mf_h, mf_w
VMF3_grid	Niell [11], Kouba [17], and Landskron and Boehm [18]	$\theta, d_{\mathrm{mjd}}, h, \phi, \lambda_{,\ \mathrm{VMF3\ gridded\ file,\ orography\_ell\ file}}$	mf_h, mf_w, zhd, zwd

ϕ and λ represent the station latitude and longitude, h represents the altitude of station, DOY represents the day of year, θ is the elevation angle, P is the surface pressure, T is the surface temperature, d_{mjd} denotes modified Julian data, ERA-40 is a European Centre for Medium-Range Weather Forecasts (ECMWF) reanalysis of the global atmosphere and surface conditions over the period 1957–2002, a_h and a_w are coefficients for determining Vienna Mapping Functions (VMF1), mf_h and mf_w are hydrostatic and wet mapping functions, respectively, and zhd and zwd are zenith hydrostatic delay and zenith wet delay, respectively.

Table 2: The properties of different methods for obtaining meteorological parameter.

Methods	Reference	Spatial resolution	Input parameters	Output parameters
GPT	Boehm et al. [4]	15°	$d_{\mathrm{mjd}}, \phi, \lambda, h$	P, T, gu
GPT2	Lagler et al. [5]	$5^\circ \times 5^\circ$	$d_{\mathrm{mjd}}, \phi, \lambda, h$	P, T, dT, e, ah, aw, gu
GPT2w	Boehm et al. [7]	$5^\circ \times 5^\circ$ or $1^\circ \times 1^\circ$	$d_{\mathrm{mjd}}, \phi, \lambda, h$	P, T, dT, T_m, e, ah, aw, la, gu
GPT3	Landskron and Bohm [18]	$5^\circ \times 5^\circ$ or $1^\circ \times 1^\circ$	$d_{\mathrm{mjd}}, \phi, \lambda, h$	P, T, dT, T_m, e, ah, aw, la, gu, $G_{n\_h}, G_{e\_h}, G_{n\_w}, G_{e\_w}$

P is the pressure; T is the temperature; gu is the geoid undulation; dT is the temperature lapse rate; e is the water vapor pressure; ah and aw are the hydrostatic and wet mapping function coefficients at zero height, respectively; T_m is the mean temperature of the water vapor; la is the water vapor decrease factor; G_{n_h} and G_{e_h} are the hydrostatic north and east gradients, respectively; and G_{n_w} and G_{e_w} are the wet north and east gradients, respectively.

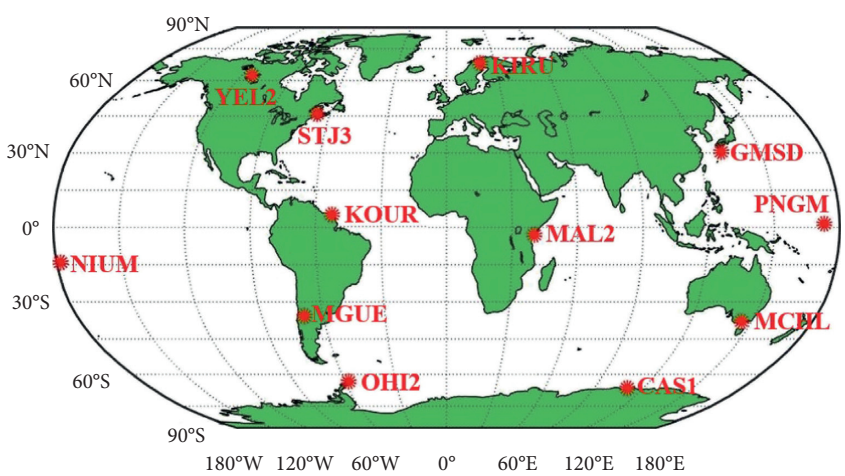

Figure 1: Geographical distribution of the 12 global MGEX tracking stations.

3.1. Influence of Different Mapping Function Models. Root mean square error (RMSE) of the difference between the calculated tropospheric delay and the tropospheric delay published by IGS was used as an indicator of repeatability [22]. The repeatability of the tropospheric delay derived from the average value of the repeatability calculated without the tropospheric gradient models (as a reference) and the repeatability calculated by adding the tropospheric gradient models are compared. The smaller ones represent improvements in the tropospheric delay repeatability. Then, we calculate the percentage of boosted results to the total number of calculated results, which is the percentage with improved repeatability. As shown in Figure 3, according to the same method for calculating meteorological parameters, the percentage with improved tropospheric delay repeatability calculated by different mapping function models is calculated. According to Figure 3, it can be concluded that the percentage with improved tropospheric delay repeatability calculated by the MFM3 mapping function model is the highest. No matter which method is used to calculate the

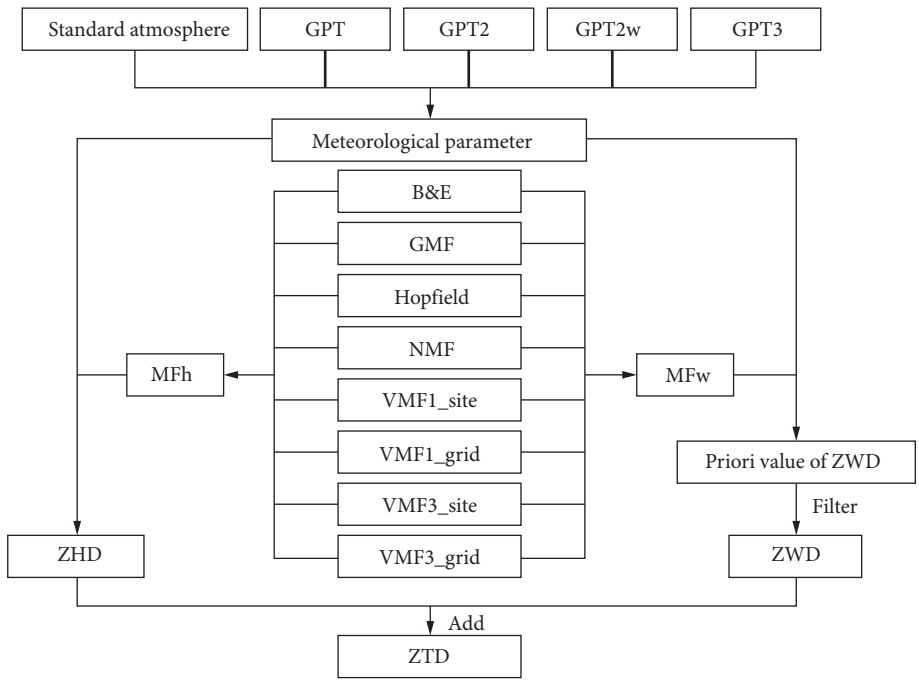

Figure 2: The processing flow of the article.

Table 3: The abbreviation of mapping function models and meteorological parameter calculation methods.

Abbreviation	Item
MFM1	B&E
MFM3	Hopfield
MFM5	VMF1_site
MFM7	VMF3_site
MFM9	VMF3_grid 5° × 5°
MP2	GPT
MP4	GPT2_1w
MP6	GPT3_1
MFM2	GMF
MFM4	NMF
MFM6	VMF1_grid
MFM8	VMF3_grid 1° × 1°
MP1	Standard atmosphere
MP3	GPT2
MP5	GPT2_5w
MP7	GPT3_5

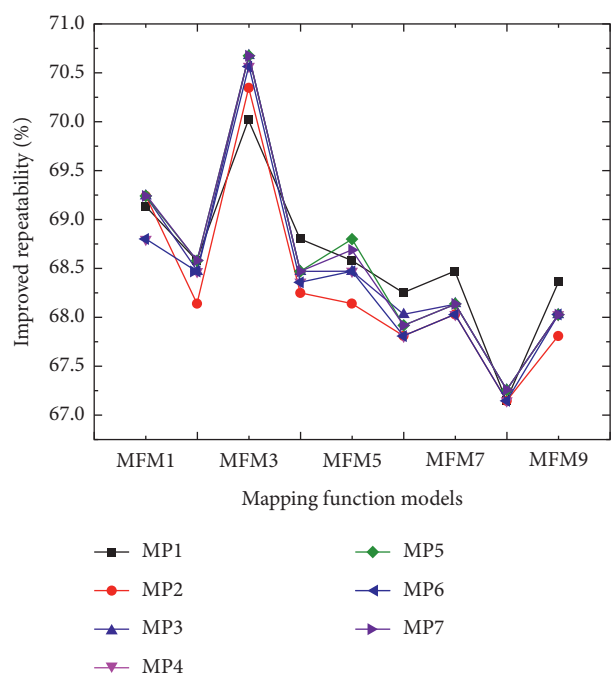

Figure 3: The percentage with improved tropospheric delay repeatability calculated by different mapping function models.

meteorological parameters, the percentage with improved repeatability is above 70%. The MFM8 mapping function model calculates the tropospheric delay improvement with the lowest repeatability percentage, and the improved repeatability percentage is below 67.5%. Regardless of the method used to calculate the meteorological parameters, the MFM2 and MFM4 mapping function models have almost the same percentage of repeatability. The repeatability of improved percentage of MFM7, MFM8, and MFM9 calculation results is not the highest; this may be due to the fact that the tropospheric gradient model has little influence on the calculation of tropospheric delay.

The repeatability of the positioning results is calculated based on the RMSE of the three directions of E, N, and U. The reproducibility of the E, N, and U directions calculated by different mapping functions refers to the comparison of the repeatability of the calculations with the tropospheric gradient models and the average of the repeatability without the tropospheric gradient models. If the latter is larger than the former, it is regarded as promoting; otherwise, it is regarded as not promoting. As shown in Figure 4, on the whole, the percentage of improved

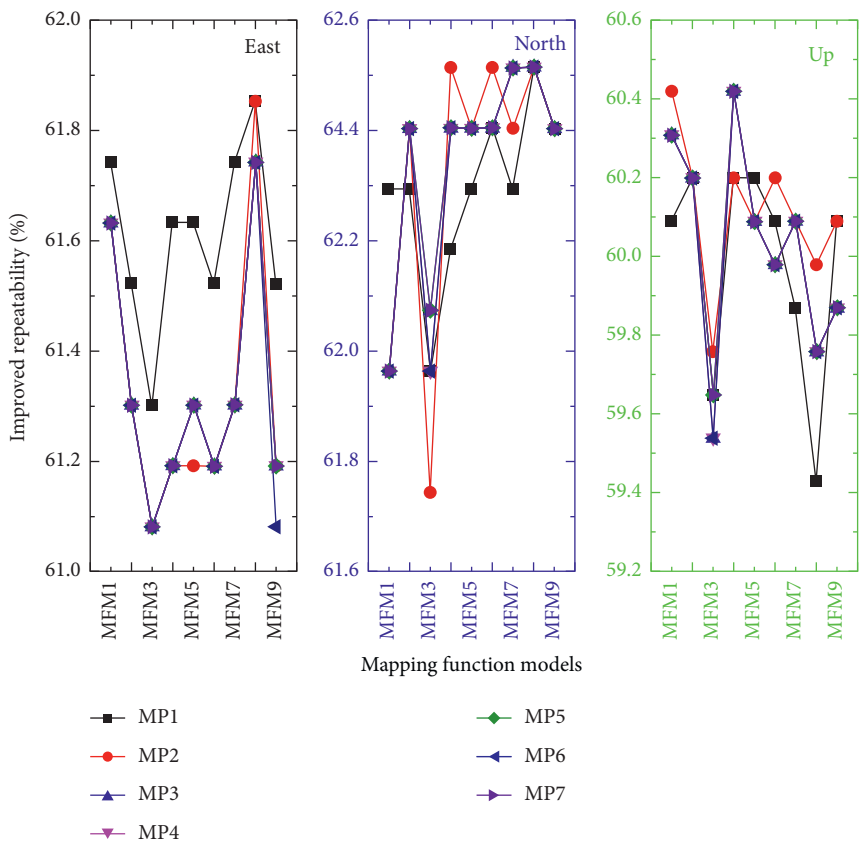

Figure 4: The percentage with improved position repeatability calculated by different mapping function models.

repeatability in the N direction is the highest and that in the U direction is the lowest. In the E direction, the percentage of the repeatability of the MFM8 mapping function model is the highest and the MFM3 mapping function model is the lowest. On the whole, under the standard atmospheric environment, the percentage of the reproducibility of the calculated results after adding the troposphere gradient model in the E direction is higher than that of other calculation methods of atmospheric parameters, which also shows that the effect is more obvious. In the method of obtaining atmospheric parameters in the N direction, except for the standard atmospheric environment, the percentage of the repeatability of the calculation results of the MFM7 and MFM8 mapping function models is the highest overall. The percentage with the improved repeatability of MFM5, MFM6, and MFM9 is almost the same, and the lowest overall improvement in repeatability is using the MFM3 mapping function model. In the U direction, the highest percentage of repeatability is the MFM4 mapping function model and the lowest percentage of repeatability is the MFM3 mapping function model.

3.2. Influence of Different Meteorological Parameter Calculation Methods

3.2.1. Improved Repeatability Percentage without Correction of Tropospheric Gradient Compared to Standard Atmospheric Parameter Model. Without the correction of the gradient model, in order to calculate the reproducibility percentage of other meteorological parameter calculation methods compared with the standard atmospheric parameters, the average RMSE of the calculation results of the standard atmospheric parameters is used as a reference. If the average RMSE of the former is smaller than the latter, then the repeatability percentage is considered to be improved. Then, we compare the number of improved repeatability to the total repeatability to obtain the improved repeatability percentage. Figure 5 shows the percentage of tropospheric delays calculated by other meteorological parameter calculation methods compared with standard atmospheric parameters without adding the tropospheric gradient models. It can be seen from Figure 5 that the percentage with the improved tropospheric delay repeatability calculated by the meteorological parameters using the MP2 method is higher than that of other meteorological parameter calculation methods, except when calculated using the MFM1 mapping function model. When using the MP3, MP4, MP5, MP6, and MP7 methods to obtain meteorological parameters to calculate the tropospheric delay, the percentage with the improved repeatability is the same when using the MFM1, MFM2, MFM3, MFM4, MFM5, and MFM7 mapping function models, and when using MFM6 and MFM9 mapping function models, the percentage with the improved repeatability reduced in turn; however, when using the MFM8 mapping function model, the percentage of improved repeatability is the lowest and fluctuates.

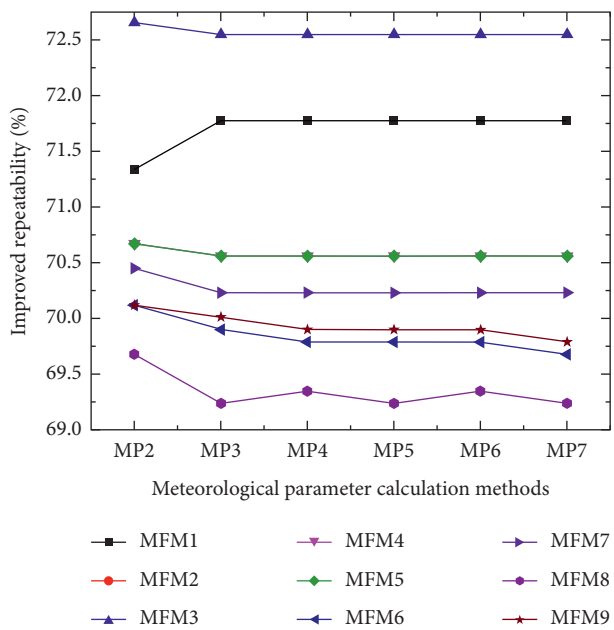

Figure 5: The percentage with improved tropospheric delay repeatability calculated by different meteorological parameter calculation methods.

It can be concluded from Figure 6 that for other meteorological parameter calculation methods without a tropospheric gradient, the percentage of the improved repeatability in the E direction is the highest, and the percentage of the improved repeatability in the U direction is the lowest. In the E direction, MP2, MP3, MP4, MP5, MP6, and MP7 have the same percentage of repeatability when using the MFM1, MFM2, MFM7, MFM8, and MFM9 mapping function models, and when using the MFM3, MFM4, MFM5, and MFM6 mapping function models, the maximum percentage of the improved repeatability does not exceed 0.3%. When using the MFM1, MFM2, MFM5, MFM6, MFM7, MFM8, and MFM9 mapping function models in the N direction, the percentage of the improved repeatability is the same, and when using the MFM3 and MFM4 mapping function models, the maximum percentage of improved repeatability does not exceed 0.3%. When using the MFM1, MFM2, MFM6, and MFM7 mapping function models in the U direction, the percentage of improved repeatability is the same, and when using the MFM3, MFM4, MFM5, MFM8, and MFM9 mapping function models, the maximum percentage of improved repeatability does not exceed 0.2%. In general, no matter which meteorological parameter calculation method and mapping function model are used, the other meteorological parameter calculation methods have substantially the same repeatability percentage compared to standard atmospheric parameters.

3.2.2. The Percentage of Improved Repeatability of Adding Tropospheric Gradient Model Compared to Standard Atmospheric Parameter Models. When calculating the tropospheric gradient and other meteorological parameter calculation methods to increase the repeatability percentage compared to the standard atmospheric parameter model, the average RMSE of the tropospheric delay or positioning result calculated by the standard atmospheric parameter model with the tropospheric gradient model is used as the reference value. If the average RMSE of the tropospheric delay or positioning result calculated by adding the tropospheric gradient of other meteorological parameters is smaller than the average RMSE calculated under standard atmospheric parameters, it is regarded as an improved repeatability, and then the number of the improved repeatability is compared to the total repeatability to obtain an improved repeatability percentage. Figure 6 shows the percentage of tropospheric delays calculated by other meteorological parameter calculation methods to improve the repeatability compared with standard atmospheric parameters with the addition of tropospheric gradient. It can be concluded from Figure 7 that the repeatability percentage of the tropospheric delay increase calculated by the meteorological parameters by the MP2 method is higher than that of other meteorological parameter calculation methods. When using MP3, MP4, MP5, MP6, and MP7 methods to obtain the meteorological parameters to calculate the tropospheric delay, the percentage of the improved repeatability is the same when using the MFM1, MFM2, and MFM6 mapping function models, and when using the MFM3, MFM4, MFM5, MFM7, and MFM9 mapping function models, the percentage of repetitiveness improved in the function model and has fluctuations, but the maximum fluctuation does not exceed 0.2%, and when the MFM8 mapping function model is used, the percentage of improved repeatability is the lowest and fluctuated.

From Figure 8, it can be concluded that compared with the standard atmospheric parameters, the method for calculating other meteorological parameters added to the gradient model has the highest reproducibility percentage in the N direction and the lowest reproducibility percentage in the U direction. In the E direction, MP2, MP3, MP4, MP5, MP6, and MP7 have the same percentage of reproducibility when using the MFM1, MFM2, MFM4, MFM6, MFM7, and MFM8 mapping function models, and when using the MFM3, MFM5, and MFM9 mapping function models, the maximum repeatability percentage increase does not exceed 0.3%. When using the MFM1, MFM2, MFM5, MFM6, MFM8, and MFM9 mapping function models in the N direction, the percentage of improved repeatability is the same, and when using the MFM3, MFM4, and MFM7 mapping function models, the maximum repeatability percentage improvement does not exceed 0.3%. In the U direction, only the repeatability percentage improved when using the MFM9 mapping function model, and the maximum percentage of improved repeatability when using the MFM1, MFM2, MFM3, MFM4, MFM5, MFM6, MFM7, and MFM8 mapping function models does not exceed 0.3%. In general, no matter which meteorological parameter calculation method and mapping function model are used, other meteorological parameter calculation methods added to the gradient model have substantially the same percentage of improved repeatability compared to standard atmospheric parameters.

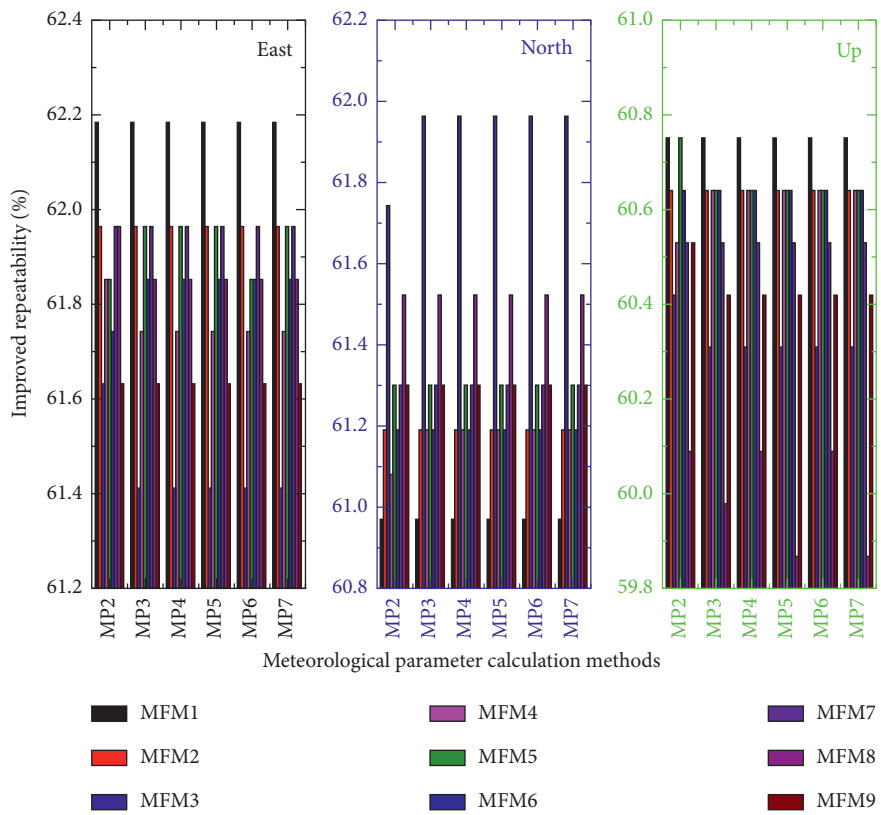

Figure 6: The percentage of repeatability improvement in positioning results calculated by different meteorological parameter calculation methods.

3.2.3. The Percentage of Improved Repeatability of Adding Tropospheric Gradient Correction Model Compared to Nontropospheric Gradient Model. When calculating the improved reproducibility percentage of the meteorological parameter calculation method with and without correction of the tropospheric gradient models, it is the tropospheric delay or positioning result calculated by meteorological parameters without correction of the tropospheric gradient model that is considered as the reference value. If the meteorological parameter calculation method corrected by the tropospheric gradient model is added, the average RMSE of the tropospheric delay or positioning result is smaller than the average RMSE of the meteorological parameters calculated without the correction of the tropospheric gradient model, and then the number of improved repeatability is compared with the total repeatability to obtain the improved repeatability percentage. Figure 9 depicts the relationship between the calculation method of different meteorological parameters with and without tropospheric gradient models and the improved repeatability percentage of tropospheric delay. It can be seen from Figure 9 that in addition to using MP1, MP2, and MP3 meteorological parameter calculation methods in the MFM1 and MFM8 mapping function models, the repeatability percentage fluctuation is small, and in other mapping function model calculation results, the repeatability percentage fluctuations are large, up to about 1.5%. For MP3, MP4, MP5, MP6, and MP7, the calculation methods for these meteorological parameters use the MFM2, MFM3, MFM4, MFM7, MFM8, and MFM9 mapping function models, respectively, and the percentage of the improved repeatability does not change much. For MP3,

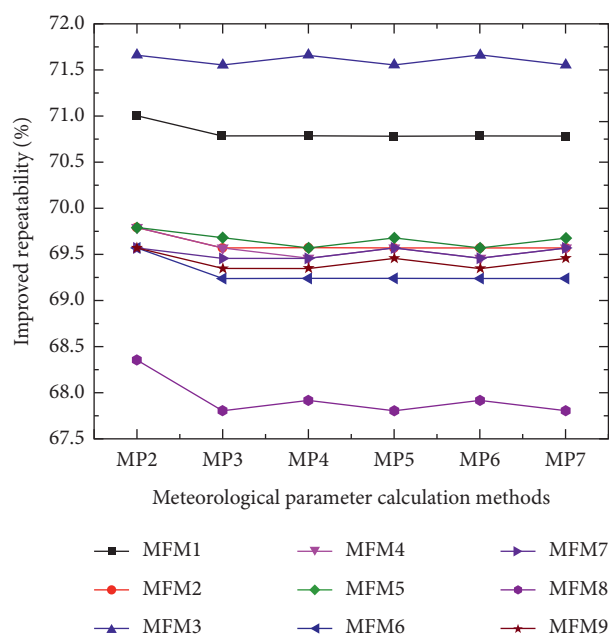

Figure 7: The percentage of improved repeatability of tropospheric delay calculated by different meteorological parameter calculation methods.

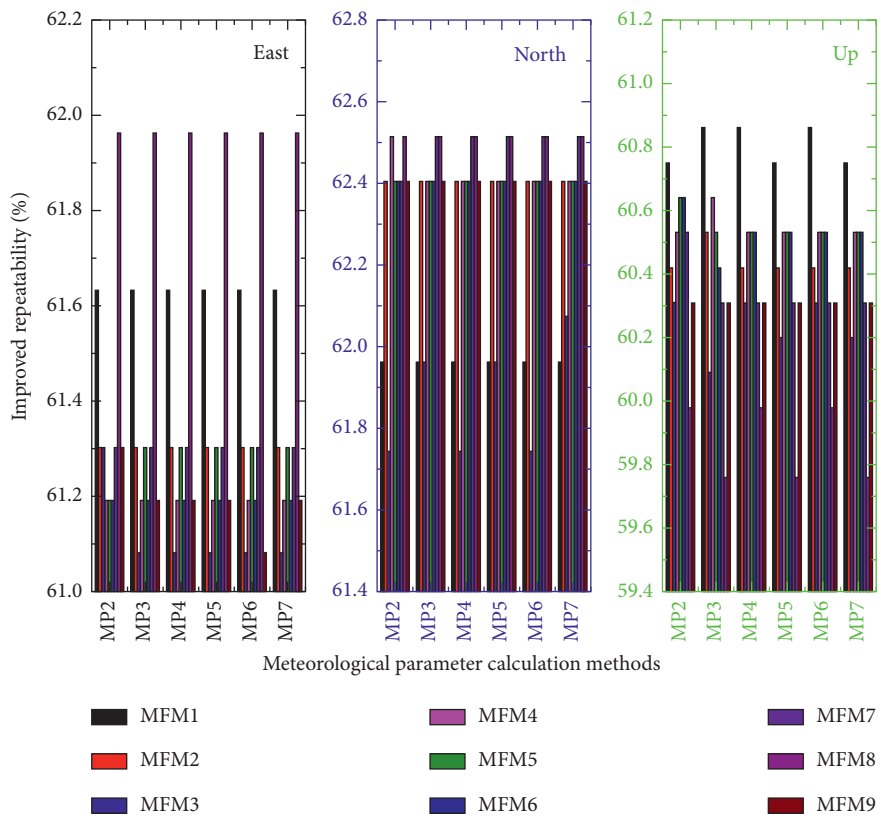

Figure 8: The percentage of improved repeatability in positioning results calculated by different meteorological parameter calculation methods.

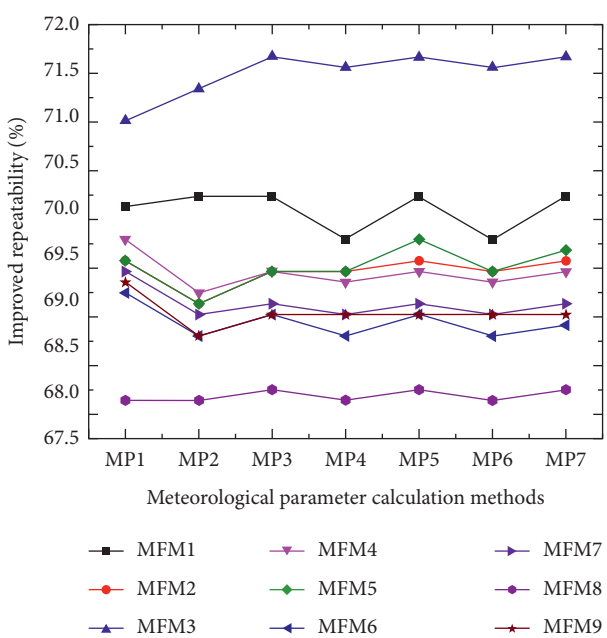

Figure 9: The percentage of improved repeatability of tropospheric delay enhancement calculated by different meteorological parameter calculation methods.

MP4, MP5, MP6, and MP7, the calculation methods for these meteorological parameters use the MFM1, MFM5, and MFM6 mapping function models which have large variations in the percentage of improved repeatability. Generally speaking, when the meteorological parameter calculation methods such as MP3, MP5, and MP7 are used, the percentage of improved repeatability is the highest.

From Figure 10, it can be concluded that compared with the meteorological parameter calculation method without the tropospheric gradient model, the meteorological parameter calculation method with the tropospheric gradient model has the highest percentage of repeatability improvement in the N direction, and the percentage of improved repeatability in the U direction is the lowest. In the E direction, when MP1 is used to obtain the meteorological parameters, no matter what mapping function model is used, the repeatability percentage is the highest. When using MP2, MP3, MP4, MP5, MP6, and MP7 to obtain the meteorological parameters, respectively, using the MFM1, MFM2, MFM3, MFM4, MFM6, and MFM7 mapping function models, the percentage of improved repeatability is the same. When using the MFM5 mapping function model, the MP3 method of obtaining meteorological parameters has the lowest percentage of repeatability; MP2, MP4, MP5, MP6, and MP7 have the same repeatability percentages as those obtained by the meteorological parameter method, which are higher than those of the MP3 method. When using the MFM8 mapping function model, the percentage of repeatability of the MP2 method for obtaining meteorological parameters is the same as that of the MP1 method; however, when using MP3, MP4, MP5, MP6, and MP7 to obtain the

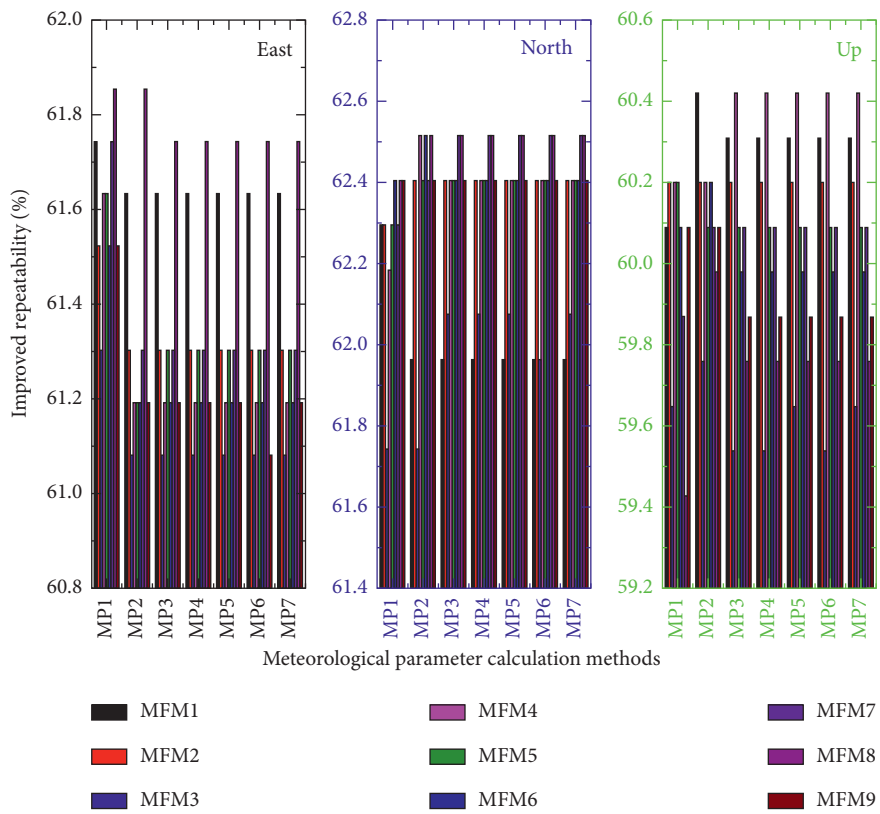

Figure 10: The percentage of improved repeatability in positioning results calculated by different meteorological parameter calculation methods.

meteorological parameter calculation method, the percentage of improved repeatability is the same but lower than the percentage calculated by the MP1 and MP2 methods. When using the MFM9 mapping function model, the MP2, MP3, MP4, MP5, and MP7 methods calculate the same percentage of improvement in reproducibility, which is lower than the percentage of improvement in MP1 and higher than the percentage of improvement in MP6. The method of obtaining meteorological parameters for MP1 in the N direction has the same and highest reproducibility when using the MFM8 and MFM9 mapping function models and the lowest reproducibility when using the MFM3 mapping function model. The method of obtaining meteorological parameters for MP2 has the same and highest reproducibility when using the MFM4, MFM6, MFM8, and MFM9 mapping function models and the lowest reproducibility when using the MFM3 mapping function model. The method of obtaining meteorological parameters for MP3, MP5, and MP7 has the highest percentage of repeatability when using the MFM7 and MFM8 mapping function models and the lowest percentage of repeatability when using the MFM1 mapping function model. The method of obtaining meteorological parameters for MP4 and MP6 has the highest percentage of reproducibility when using MFM7 and MFM8 mapping function models and the lowest percentage of repetitiveness when using MFM1 and MFM3 mapping function models. Regardless of the mapping function model used in the seven meteorological parameter calculation methods mentioned above, the difference between the maximum improved repeatability percentage and the minimum improved repeatability percentage does not differ by more than 0.6%. Except for the MP1 meteorological parameter calculation method in the U direction, when the other six meteorological parameter calculation methods are adopted, the MFM3 mapping function model has the lowest reproducibility improvement, and when using MP1, the improved repeatability percentage by the MFM3 mapping function model is the second smallest. For the MP1 meteorological parameter calculation method, using MFM2, MFM4, and MFM5 mapping function models has the highest percentage of repeatability improvement, while using MFM8 mapping function model has the lowest percentage of repeatability improvement. For the MP2 meteorological parameter calculation method, the MFM1 mapping function model has the highest percentage of repeatability improvement. For MP3, MP4, MP5, MP6, and MP7 meteorological parameter calculation methods, the MFM4 mapping function model has the highest percentage of repeatability improvement; the difference between the maximum and minimum repeatability percentage enhancements does not exceed 1%. In general, no matter what kind of meteorological parameter calculation method and mapping function model is used, the repeatability percentage of the meteorological parameter calculation method with the gradient model is substantially the same as that of the meteorological parameter calculation method without the gradient model.

4. Conclusions

GPS SF PPP is used in this paper; seven meteorological parameter calculation methods (MP1, MP2, MP3, MP4, MP5, MP6, and MP7) and nine mapping function models (MFM1, MFM2, MFM3, MFM4, MFM5, MFM6, MFM7, MFM8, and MFM9) are used to calculate the tropospheric delay and the positioning error in the three directions of E, N, and U. The following conclusions are drawn:

(1) When the same meteorological parameter calculation method is used, the percentage of improved tropospheric delay repeatability calculated by MFM3 is the highest and that calculated by MFM8 is the lowest; the percentage of improved positioning error repeatability in the N direction is the highest and that in the U direction is the lowest; the positioning error in the E direction is the highest using MFM8 and that in the N direction is the highest using MFM7 and MFM8. It has the highest percentage of improved positioning repeatability in the U direction by using MFM4, and in the E, N, and U directions when using MFM3, the percentage of improved positioning repeatability is the lowest.

(2) When the same mapping function model is used, compared with the standard meteorological parameters without the correction of the tropospheric gradient model, no matter which of the seven meteorological parameter calculation methods is used, the difference between the calculated maximum and minimum repeatability percentage of tropospheric delay improvement is less than 0.5%. The percentage of improved positioning repeatability in the E direction is the highest and that in the U direction is the lowest; the maximum difference in the repeatability percentage of the calculated positioning result improvement is less than 0.3%. It shows that different calculation methods of meteorological parameters have little effect on the calculation results.

(3) When the same mapping function model is used, the gradient model is added to compare with the standard meteorological parameters; no matter which of the seven meteorological parameter calculation methods is used, the calculated tropospheric delay increase is between the maximum and minimum repeatability, and the difference is less than 0.2%. The percentage of improved positioning repeatability in the N direction is the highest and that in the U direction is the lowest. The difference between the maximum and minimum repeatability percentages of the calculated positioning error improvement is less than 0.3%.

(4) When the same mapping function model is used, the gradient model correction is added compared with the nongradient model correction; no matter which of the seven meteorological parameter calculation methods is used, the difference between the calculated maximum and minimum repeatability of the tropospheric delay increase can be up to 1.5%; the percentage of improved positioning repeatability in the N direction is the highest, and it is the lowest in the U direction; the difference between the maximum and minimum repeatability percentages of the calculated positioning improvement is less than 0.6%. So, it shows that adding the gradient model has a greater impact on the calculation of tropospheric delay and positioning.

Data Availability

The data used to support the findings of this study are available from the IGS.

Conflicts of Interest

The authors declare that they have no conflicts of interest.

Acknowledgments

The authors thank IGS for data and the team of Feng Zhou of Shandong University of Science and Technology for the open-source software GAMP. This study was supported by the National Natural Science Foundation of China (grant nos. 41674008, 41974026, 41604006, and 41874006) and the National Key Research and Development Program of China (grant no. 2016YFB0501501).

References

[1] K. Saha, C. Suresh Raju, and K. Parameswaran, "A new hydrostatic mapping function for tropospheric delay estimation," *Journal of Atmospheric and Solar-Terrestrial Physics*, vol. 72, no. 1, pp. 125–134, 2010.

[2] B. Pace, R. Pacione, C. Sciarretta, and G. Bianco, "Computation of zenith total delay correction fields using ground-based GNSS," *International Association of Geodesy Symposia*, vol. 142, pp. 131–137, 2016.

[3] N. Penna, A. Dodson, and W. Chen, "Assessment of EGNOS tropospheric correction model," *Journal of Navigation*, vol. 54, no. 1, pp. 37–55, 2001.

[4] J. Boehm, R. Heinkelmann, and H. Schuh, "Short Note: a global model of pressure and temperature for geodetic applications," *Journal of Geodesy*, vol. 81, no. 10, pp. 679–683, 2007.

[5] K. Lagler, M. Schindelegger, J. Böhm, H. Krásná, and T. Nilsson, "GPT2: empirical slant delay model for radio space geodetic techniques," *Geophysical Research Letters*, vol. 40, no. 6, pp. 1069–1073, 2013.

[6] J. Boehm, A. Niell, P. Tregoning, and H. Schuh, "Global mapping function (GMF): a new empirical mapping function based on numerical weather model data," *Geophysical Research Letters*, vol. 33, no. 7, 2006.

[7] J. Boehm, G. Moller, M. Schindelegger, G. Pain, and R. Weber, "Development of an improved empirical model for slant delays in the troposphere (GPT2w)," *GPS Solutions*, vol. 19, no. 3, pp. 433–441, 2015.

[8] J. Saastamoinen, "Atmospheric correcton fot the troposohere and stratosphere in radio ranging satellites," *The Use of Artificial Satellites for Geodesy*, vol. 15, pp. 247–251, 1972.

[9] J. W. Marini, "Correction of satellite tracking data for an arbitrary tropospheric profile," *Radio Science*, vol. 7, no. 2, pp. 223–231, 1972.

[10] T. A. Herring, "Modeling atmospheric delays in the analysis of space geodetic data,""Modeling atmospheric delays in the analysis of space geodetic data," in *Proceedirws of Refraction of Transatmospheric Simals in Geodesy*, J. C. De Munck and T. A. Spoelstra, Eds., vol. 36, no. 4, Geodetic Commission Publications on Geodesy, Netherlands, Europe, 1992.

[11] A. E. Niell, "Global mapping functions for the atmosphere delay at radio wavelengths," *Journal of Geophysical Research: Solid Earth*, vol. 101, no. B2, pp. 3227–3246, 1996.

[12] A. E. Niell, "Improved atmospheric mapping functions for VLBI and GPS," *Earth, Planets and Space*, vol. 52, no. 10, pp. 699–702, 2000.

[13] U. Foelsche and G. Kirchengast, "A simple "geometric" mapping function for the hydrostatic delay at radio frequencies and assessment of its performance," *Geophysical Research Letters*, vol. 29, no. 10, 2002.

[14] S. A. M. Younes, "Improved dry tropospheric propagation delay mapping function for GPS measurements in Egypt," *Journal of Spatial Science*, vol. 59, no. 2, pp. 181–190, 2014.

[15] H. D. Black and A. Eisner, "Correcting satellite Doppler data for tropospheric effects," *Journal of Geophysical Research*, vol. 89, no. D2, p. 2616, 1984.

[16] H. S. Hopfield, "Two-quartic tropospheric refractivity profile for correcting satellite data," *Journal of Geophysical Research*, vol. 74, no. 18, pp. 4487–4499, 1969.

[17] J. Kouba, "Implementation and testing of the gridded Vienna mapping function 1 (VMF1)," *Journal of Geodesy*, vol. 82, no. 4-5, pp. 193–205, 2008.

[18] D. Landskron and J. Böhm, "VMF3/GPT3: refined discrete and empirical troposphere mapping functions," *Journal of Geodesy*, vol. 92, no. 4, pp. 349–360, 2018.

[19] F. Zhou, D. N. Dong, M. R. Ge, P. Li, J. Wickert, and H. Schuh, "Simultaneous estimation of GLONASS pseudorange interfrequency biases in precise point positioning using undifferenced and uncombined observations," *GPS Solutions*, vol. 22, no. 1, 2018.

[20] R. Wang, J. Gao, N. Zheng et al., "Research on accelerating single-frequency precise point positioning convergence with atmospheric constraint," *Applied Sciences*, vol. 9, no. 24, p. 5407, 2019.

[21] Z. Liu, M. S. Wong, J. Nichol, and P. W. Chan, "A multisensor study of water vapour from radiosonde, MODIS and AERONET: a case study of Hong Kong," *International Journal of Climatology*, vol. 33, no. 1, pp. 109–120, 2013.

[22] F. Zhou, X. Li, W. Li et al., "The impact of estimating high-resolution tropospheric gradients on multi-GNSS precise positioning," *Sensors*, vol. 17, no. 4, p. 756, 2017.

[23] G. Chen and T. A. Herring, "Effects of atmospheric azimuthal asymmetry on the analysis of space geodetic data," *Journal of Geophysical Research: Solid Earth*, vol. 102, no. B9, pp. 20489–20502, 1997.

[24] F. Zheng, Y. Lou, S. Gu, X. Gong, and C. Shi, "Modeling tropospheric wet delays with national GNSS reference network in China for BeiDou precise point positioning," *Journal of Geodesy*, vol. 92, no. 5, pp. 545–560, 2018.